

Convolutional neural network for assisting accuracy of personalized clavicle bone implant designs

Dita Ayu Mayasari¹, Ihtifazhuddin Hawari^{1,2}, Sheba Atma Dwiyantri¹, Nathasya Reinelda Noviyadi¹, Dinda Syaqla Andryani¹, Muhammad Satrio Utomo^{3,4}, Nada Fitriyatul Hikmah⁵, Talitha Asmaria⁶

¹Department of Biomedical Engineering, Faculty of Engineering, University of Dian Nuswantoro, Semarang, Indonesia

²Department of Electrical Engineering, Faculty of Engineering, Diponegoro University, Semarang, Indonesia

³Research Center of Metallurgy, Research Organization of Nanotechnology and Materials, National Research and Innovation Agency (BRIN), South Tangerang, Indonesia

⁴Department of Biomedical Engineering, University of Melbourne, Victoria, Australia

⁵Department of Biomedical Engineering, Institute Technology of Sepuluh November, Surabaya, Indonesia

⁶Center of Biomedical Research, Research Organization of Health, National Research and Innovation Agency (BRIN), Bogor, Indonesia

Article Info

Article history:

Received Nov 3, 2023

Revised Jan 17, 2024

Accepted Jan 23, 2024

Keywords:

Artificial intelligence

Clavicle plate

Computational aided design

Computational tomography

Image classification

ABSTRACT

The clavicle is a long bone that tends to be frequently fractured in the midshaft region. The plate and screw fixing method is mainly applied to address this issue. This study aims to construct a clavicle bone implant design with a consideration to achieve a high accuracy and high-quality surface between the plate and the clavicle surface. The computational tomography scanning (CT-scan) image series data were processed using a convolutional neural network (CNN) to classify the clavicle image. The CNN outcomes were gathered as three-dimensional (3D) volume data of clavicle bone. This 3D model was then proposed for the plate design. The CNN testing results of 97.4% for the image clavicle bones classification, whereas the prints of the 3D model from clavicle bone and its plate and screw design reveal compatibility between the bone surface and the plate surface. Overall, the CNN application to the series of CT images could ease the classification of clavicle bone images that would precisely construct the 3D model of clavicle bone and its suitable clavicle bone plate design. This study could contribute as a guideline for other bone plate areas that need to fit the patient's bone geometry.

This is an open access article under the [CC BY-SA](https://creativecommons.org/licenses/by-sa/4.0/) license.



Corresponding Authors:

Dita Ayu Mayasari

Department of Biomedical Engineering, Faculty of Engineering, University of Dian Nuswantoro

Semarang, Indonesia

Email: mayasari.dita@dsn.dinus.ac.id

1. INTRODUCTION

The clavicle, also known as the collarbone, is a long bone which connects the axial and appendicular skeleton to the scapula. It has a sigmoid-shaped and convex surface from a cephalad position [1]. The clavicle is a supporting bone that functions for lateral fixation of the arm so it can move freely. The clavicle is reported to be the most often fractured bone. From 2001 to 2020, a total of 17.089 clavicle fracture operations were done in Australia [2]. There are three types of clavicle fractures: midshaft, lateral, and medial fractures. Midshaft fractures were the most prevalent, accounting for 69% to 82% of all cases. The terminology of midshaft clavicular fractur is referred to an area on the middle third of the clavicle. This area is most prone to acute injury because the thinnest section of the clavicle and lacks reinforcing support from muscle and ligamentous attachments [3]. This condition should be fixed quickly to restore the upper extremity function while avoiding impairment [4]. There are three possibilities for midshaft clavicular fractur

treatment: non-surgical treatment, intramedullary nailing (IMN), and plate and screw fixation. Nonsurgical treatment has a high chance of failure for clavicular fractures with prominent displacement and significant comminution [5]. Although IMN looked to have fewer wound problems, plate and screw fixation were found to be more effective than IMN in preventing malunion. Plate and screw fixation were more suggested for malunion prevention [6].

Plate design plays a pivotal role in preventing fixation failure [7]. Specific morphologies of bones and fracture types require specific designs of plates [8]. The fitness between plate design and bone morphology can be obtained using the reverse engineering (RE) method. This method was used to construct the three-dimensional (3D) model of bone [9]. Furthermore, the obtained 3D bone model could be functioned to generate a new plate shape [10]. 3D bone model acquisition can be done using computed tomography scan (CT-scan) which produces many slices of images. Creating individualized osteo-clavicular implant planning from CT-scan images is a time-consuming on region of interest (ROI) segmentation procedure [11]. Based on several literatures, the application of artificial intelligence, particularly using convolutional neural network (CNN) could ease the selection of the ROI. Particular researches have detected the ROI, particularly the tooth image from dental panoramic radiography (DPR) and nine different total hip replacement (THR) implant designs [12], suspected a failure [13], from 402 plain image radiography using CNN, combined with additional techniques [14]. In their conclusions, both totally agree that CNN produced high speed and high accuracy to detect the interest of their studies. Moreover, a surgical procedure in China has employed CNN to prepare the segmentation process from plenty digital imaging and communications in medicine (DICOM) images, which if it is done manually by radiologist will take more than two days [15]. The final segmentation process took only one minute to separate the tumor region from the whole surround area in the lower abdomen CT-scan image. It then could assist further plans for a customized implant design for a real case of pelvic tumor patient. Overall, CNN is a very promising technique to advance many medical conditions and solutions, including the personal request for reaching a higher success rate during operation.

This study aims to employ the CNN approach to perform autonomous classification of slice which conduct bone target. Although there are already CNN applications for many types of implant design. However, to the best of our knowledge, this research is a novel work that attempts to design a clavicle bone implant design using CNN with a target of a high accuracy that could mimic the surface on the patient's clavicle bone.

2. METHOD

In this research, DICOM data which consist of 1,394 slices of CT-scan images of the male thorax. The data was acquired from Saiful Anwar General Hospital. This study consisted of five main stages: data pre-processing, the clavicle image classification, the clavicle image segmentation, the clavicle image reconstruction and refinement, and the clavicular plate design stage.

2.1. Pre-processing CT-scan data

First, the obtained CT-scan data was processed to improve the image quality by obtaining pixel image data from DICOM data and translate it to Hounsfield Units (HU). HU has a normalized X-ray attenuation index in DICOM data that is based on a scale of 21,000 for air and 0 for water at standard pressure and temperature [16]. The conversion consists of 40 to 80 HU for soft tissue and 800 to 1,500 for hard tissue. To enhance the figure of the bone image, it employed dilatation morphology and changed the gray image to a binary image of 512×512 pixels. Figure 1 shows the pre-processing from the original data to the bone image.

2.2. Clavicle image classification

The purpose of image classification is to separate the images that contain only clavicle bone. The following step was data augmentation, which included rescaling pixel sizes, rotating images, mirroring images, zooming images, and creating data batches of four image files each. These parameters are delivered in Table 1. After that, the training configuration was started. The dataset was labeled with two labels: clavicle and non-clavicle. Each label's data was split into 75% for training and 25% for testing. This division provided 975 data for training and 419 for testing. After splitting the data, the pixel size was rescaled to 256×256 to minimize the computing complexity in the classification process [17].

The classification process was carried out using CNN. The CNN network design, shown in Figure 2, was made up of 19 layers: convolutional layers, max pooling layers, flattening layers, dense layers, and dropout layers. The convolutional layer's filter is 3×3 with a two-stride shift [18]. Max pooling functions to reduce by half the pixel size every time a new layer is entered. The architecture's dropout was set at 0.25. Afterwards, the Adam optimizer was implemented to optimize the training process on the CNN architecture. In architecture, the loss function matrix employs binary cross-entropy. In this study, configuring the

hyperparameters implies determining the batch size, learning rate, step size, and epoch, delivered in the Table 2. The result from CNN expects to separate the figure in folders based on their categories, those are clavicle and non-clavicle.

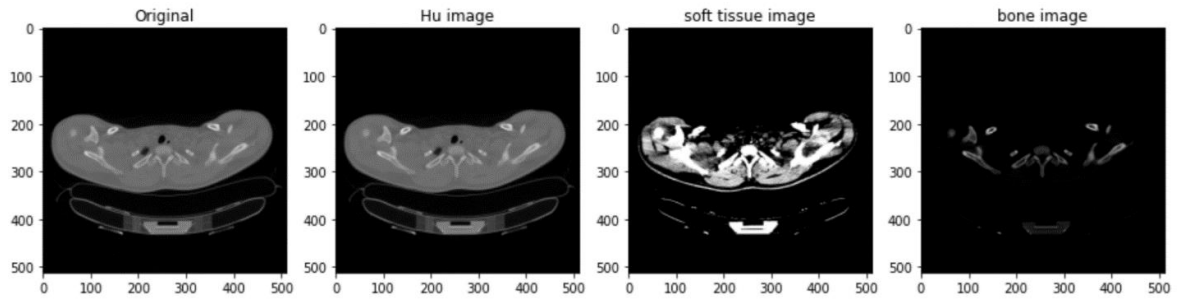


Figure 1. A series of pre-processing data from the original CT-scan image to the separated bone image

Table 1. Data augmentation parameters

Rescaling	Rotating	Mirroring	Zooming	Fill mode	Batch size
1/255	60°	Vertical & Horizontal	0.2	nearest	4

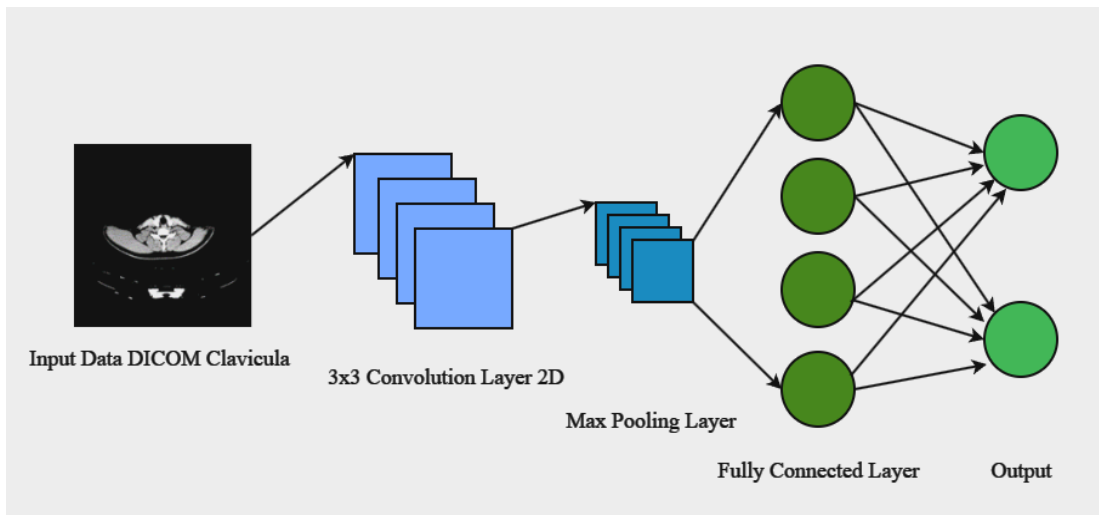


Figure 2. CNN architecture

Table 2. Hyperparameter tuning

Optimizer	Learning rate	Step size	Batch size	Epoch
Adam optimizer	1×10^{-5}	338	4	50

CNN architecture evaluation made in this study is to use accuracy and confusion matrix calculations. Calculation of accuracy by calculating the number of y_{true} (original target) that is equal to y_{pred} (predicted result) divided by the data used in the architectural training process. The formulation of the accuracy calculation is as in (1). The confusion matrix in this architecture is precision, recall, and F1-Score. Precision is the percentage of correct predictions of a class among all predictions for that class. Recall is the proportion of correct predictions from a class and the total number of occurrences of that class. F1-Score is a combination of precision and recall.

$$Accuracy = \frac{\sum_{i=1}^n y_{true} == y_{pred}}{n} \tag{1}$$

2.3. Clavicle image segmentation

The input data for the clavicle image segmentation step was collected from the classified picture folder that was included in the “clavicle” class in DICOM format. This step employed MATLAB and the tool of “image segmenter” function to execute the image segmentation. After loading the data, it was transformed into a 512×512 pixel matrix using the uint8 data type. The intensity value in the grayscale image was then mapped to produce a new value of this data. Lastly, the “graph cut” tool was used to determine the foreground and background sections of the image. The segmentation procedure in image data processing is used to separate or identify various regions of an image [19]. The segmentation procedure was employed in this work to distinguish the clavicle from the thorax. To identify the item, gather the pixels that comprise the clavicle and segregate the non-clavicular from the thorax [20].

After that, the images were masked with per-slice image data and proceeded with thresholding to get the final segmentation result, which was binary image data. The threshold level was employed as the threshold method. The graythresh function would be used to calculate the threshold value, with the normal value range being [0.1]. Figure 3 shows clavicle image segmentation stages from foreground and background determination.

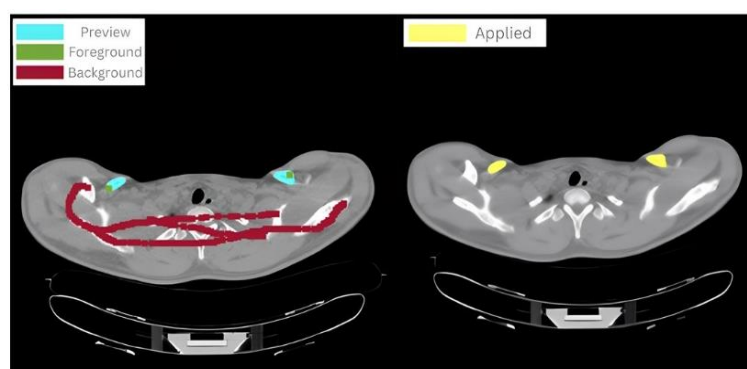


Figure 3. Clavicle image segmentation consists of determining the foreground and background (left image) and the determination of clavicle bone with yellow color (right image)

2.4. Clavicle image reconstruction and refinement

The segmented image from each slice was collected into a single folder and then visualized in 3D. This 3D visualization approach used the rendering method and involved transformation and interaction with multi-dimensional biomedical image data sets. There was no requirement for surface discretization on rendering volumes, hence image data integrity was well preserved. Despite the lengthy computing time, this approach could provide a high-quality image presentation. Image data from segmentation findings would be represented in 3D volume data using the ImageJ application and loaded in the 3D viewer software. After that, since the data still has some trash around the clavicle bone, the image refinement using Autodesk PowerShape Student Licensed was employed. Figure 4 shows the clavicle bone image that has been reconstructed but still requires refinement.

2.5. Clavicular plate design

The clavicle used was the left clavicle, with the implant plan placed on the superior side. Fusion 360 computer-aided design (CAD) software was used to create this design. The first step was to take the clavicle bone's midplane. This phase was completed by using the extrude feature to remove the clavicle bone ends. The last step was to create a plate using the surface contour in the superior region. This was accomplished by applying the loft feature to the clavicle bone's surface. It was then sliced in half to create a plate pattern that matched the surface shape of the clavicle bone. Figure 5 shows all processes in bone plate design, consisting of clavicle bone reconstruction in Figure 5(a), clavicle bone removal in Figure 5(b) and surface contouring for customized plate designs in Figure 5(c).

The next step was to create the screw holes. On the inside surface of the plate, a circle with an outside diameter of 10 mm and an internal diameter of 4 mm was sketched. Then, use the rectangular pattern feature to make four holes 24 mm apart. After that, an intersecting pattern circle was created with the body plate to form a hole that conforms to the contour of the plate surface. The following step was to use the fillet function to round the edges of the body plate. The bone screw design was referred to ISO 5835:1991, the

thread size is 4 mm, and the screw head thickness is 2.4 mm. It is ISO-approved for metal bone screws with a hexagonal drive joint; the bottom face of the head is spherical with an asymmetrical thread [21]. Figure 6 shows the screw holes design process, consists of constructing the rectangular pattern for preparing the hole designs in Figure 6(a), composing other holes using an intersecting pattern circle in Figure 6(b) and building the plate surface contour in Figure 6(c).

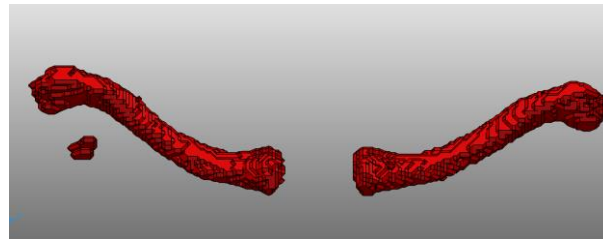


Figure 4. Clavicle image reconstruction requires a refinement process

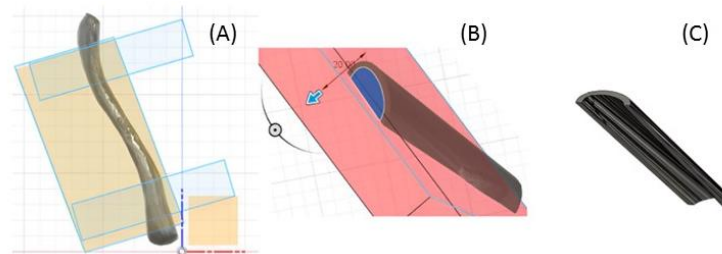


Figure 5. Clavicle plate design process: (a) the midplane of the clavicle bone construction using the extrude feature, (b) the clavicle bone removal, and (c) producing a plate using the surface contour in the superior region

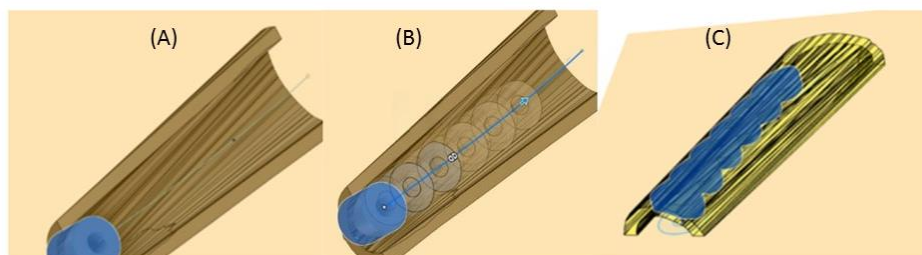


Figure 6. The process of designing screw holes by creating hole with an outside and an internal diameter: (a) employing the rectangular pattern feature to make six holes, (b) and lastly composing an intersecting pattern circle with the body plate to form a hole, and (c) conforms to the contour of the plate surface

3. RESULTS AND DISCUSSION

The clavicle image pre-processing was done to strengthen the bone image from all over the obtained CT-scan data. Besides improving the image quality, the pre-processing could remove noise or interference, and alter the image to meet the requirements of a specific analysis or application [22]. The final result from the image pre-processing step is binary images, presented in Figure 7.

The clavicle image classification steps employed a CNN architecture with a variant of the U-Net CNN architecture. The U-Net architecture has been taught to perform equivalent, if not better, multi-class clavicle segmentation. To train all tissues, there are two approaches: single-class (train tissue to segment into only one organ, requiring all DICOM data to segment the clavicle) and multi-class (train networks on DICOM data to segment the clavicle) [23].

At each layer of the CNN architecture, a ReLU activation function is applied. It attempts to introduce non-linearity throughout the network. During the convolution process, the image's size will steadily decrease while the number of filters or features detected will increase [24]. In the convolutional layer, dense layer 16, ReLU activation was employed. Since the CNN architecture was utilized to identify only two labels, clavicle and non-clavicle, the activation function in dense layer one used sigmoid activation [25], [26].

Overall, the training part took 44.65 minutes for the processing of the data duration, whereas the testing took only 30 seconds. By computing the (1), the results of 75%, or 975 training data show it has good accuracy, with a loss value is 0.0857. As a result, using a trained network, the classification results can determine the class of clavicle with an average accuracy of 95.37%. Next, the CNN architecture is used to test the rest of the 25% or 419 testing data. The test results show an accuracy of up to 97.4%. Figure 8(a) showed the training and validation losses have significantly dropped for epochs under 10, which means the model could start to understand the dataset that was used during training and validation. It is in opposition to Figure 8(b) for the training and validation accuracy picture, where the line has been rapidly increasing for epochs less than 10. It implies that the accuracy would rise as a result of the model's ability to comprehend the dataset. Based on Table 3, the accuracy for training is 95.3% while for testing is 97.4%.

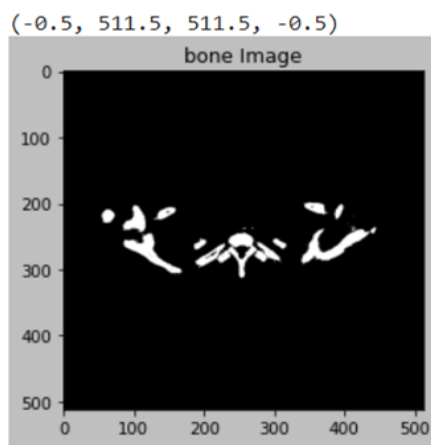


Figure 7. Clavicle image pre-processing results in binary data

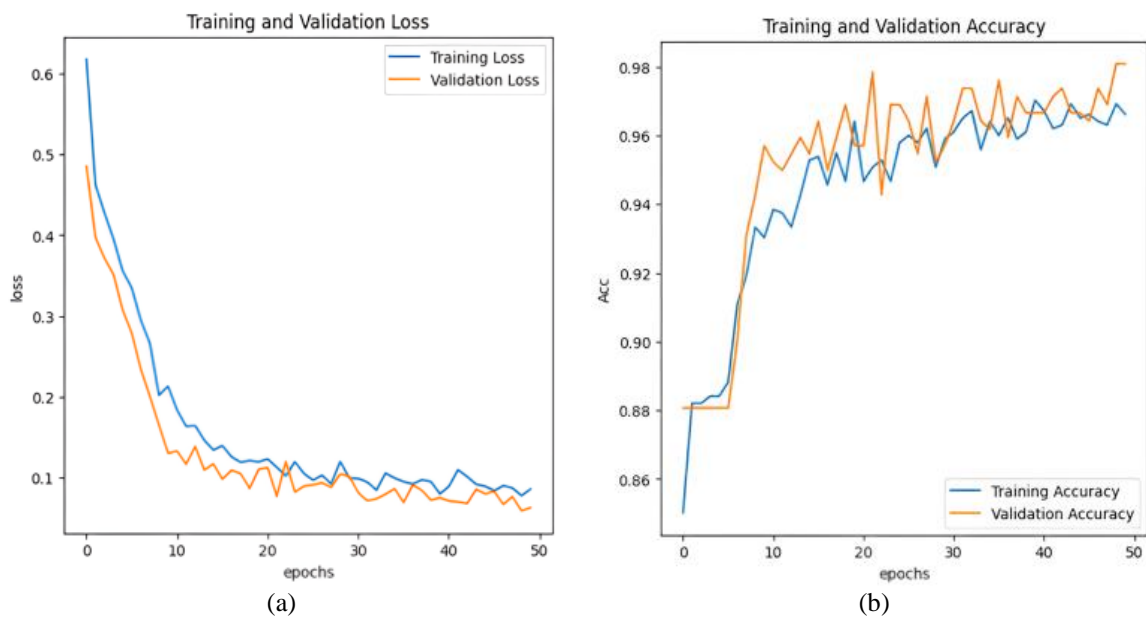


Figure 1. The results of the prediction model training and validation loss process: (a) the results of the prediction model training and (b) validation accuracy process

Table 3. Confusion matrix

		Precision	Recall	F1-Score
Training	Clavicula	0.860	0.933	0.895
	Non Clavicula	0.991	0.980	0.985
	Accuracy			0.953
Testing	Clavicula	0.925	0.956	0.940
	Non Clavicula	0.975	0.974	0.975
	Accuracy			0.974

The clavicle image segmentation has been successfully conducted by obtaining clavicle-labeled images via CNN to produce the collarbone images. Figure 9(a) shows the clavicle bone image segmentation on one slice. In the clavicle image reconstruction, the 3D clavicle bone model is performed to build an accurate and realistic model from DICOM thorax data [27]. Objects discovered by the clavicle during the previous segmentation phase can now be turned into a more complicated 3D model by merging the numerous sides and components identified by the clavicle. This technique is like triangulation in that it combines pixels to form a nice geometric shape [28].

The volume rendering method was employed in this 3D visualization procedure, which comprises transformation and interaction with multi-dimensional biomedical picture data sets. Although there is no requirement for discretization from the surface in volume rendering, the image data's integrity is preserved. Even though it is time demanding, this process may provide high-quality image displays. Image data from segmentation was processed in this study utilizing a 3-dimensional visualization using the ImageJ tool, the results of which are shown in Figure 9(b). Overall, the clavicle images have been refined to smoothen the surface, close all appeared holes and removing the trash surround the 3D model. The refinement process result is shown in Figure 9(c).

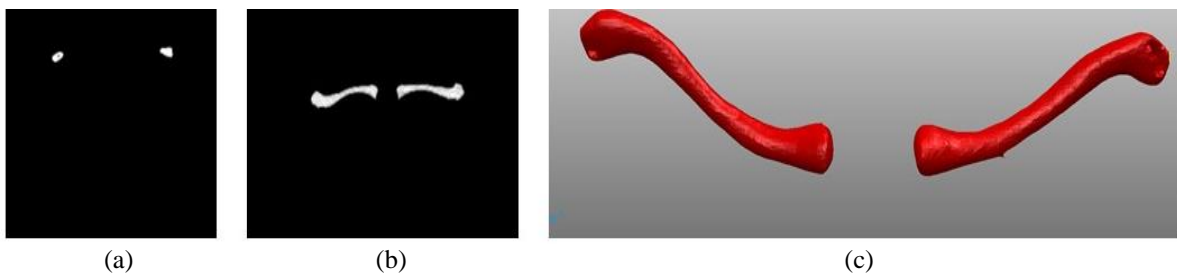


Figure 9. Result after the segmentation process: (a) in one slice, (b) in all slices, and (c) result after refinement

The validation stage was carried out by comparing the dimensions of the segmented clavicle bone to the CT scan data. Autodesk Fusion 360 software was used to measure clavicular dimensions. The morphological parameters measured were lateral-to-medial length (CL), the position of the conoid tubercles was measured from the lateral end of the clavicle (d_{CT}), half of the clavicle's apparent length ($h_{50\%}$), apparent half-length of maximal clavicle on superior view (d_{bow_sup}) and half the apparent width of the clavicle ($w_{50\%}$) [29]. The measurement technique is carried out in the anterior and posterior views, as shown in Figure 10.

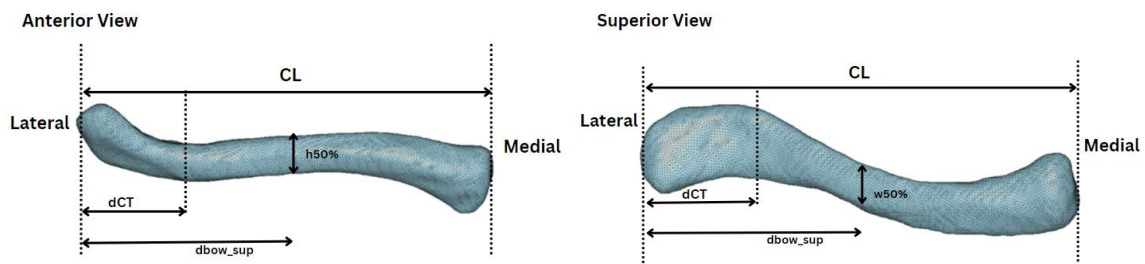


Figure 10. Measurement of the dimensions of the clavicle bone in the anterior view and superior view

The final refinement 3D clavicle bone was validated by comparing the segmented 3D clavicle bones using a software of 3D Slicer. Based on dimensional measurements, it can be determined that the results of 3D clavicle bone model performed with CNN are almost similar from those produced by segmentation performed with a 3D Slicer as shown in Table 4. There is a deviation between CT-Scan and CNN-based segmentation, about 0.01 to 0.02 cm. The previous study showed that the length of clavicle is around 152 to 156 mm for male and 105-117 mm for female, while the mid-shaft circumference was around 4 to 6 mm for male left clavicle [30].

The 3D geometry of the clavicle bone, obtained through CNN-based segmentation, was utilized in fabricating a clavicle plate implant. The left clavicle was selected for this purpose, with the implant plan intended for the superior side. Figure 11 illustrates the design of the clavicle plate based on the segmentation results of the clavicle bone using CNN. In the figure, there are three designs with holes numbered 4, 5, and 6. For the plate with 4 holes in Figure 11(a), the plate measures 34 mm in length, 3.5 mm in thickness, and has a screw hole diameter of 4mm. For the plate with hole 5 in Figure 11(b), the plate measures 45 mm in length, 3.5 mm in thickness, and also has a screw hole diameter of 4 mm. Lastly, for the plate with hole 6 in Figure 11(c), the plate measures 50 mm in length, 4 mm in thickness, and maintains a screw hole diameter of 4 mm.

Table 4. Comparison of dimension measurement

Parameter	Data CT-Scan (using 3D Slicer)	CNN-based segmentation	Deviation
CL	15.31 cm	15.30 cm	0,01
$h_{50\%}$	1.15 cm	1.15 cm	0
d_{CT}	3.97 cm	3.99 cm	0.02
d_{bow_sup}	7.50 cm	7.50 cm	0

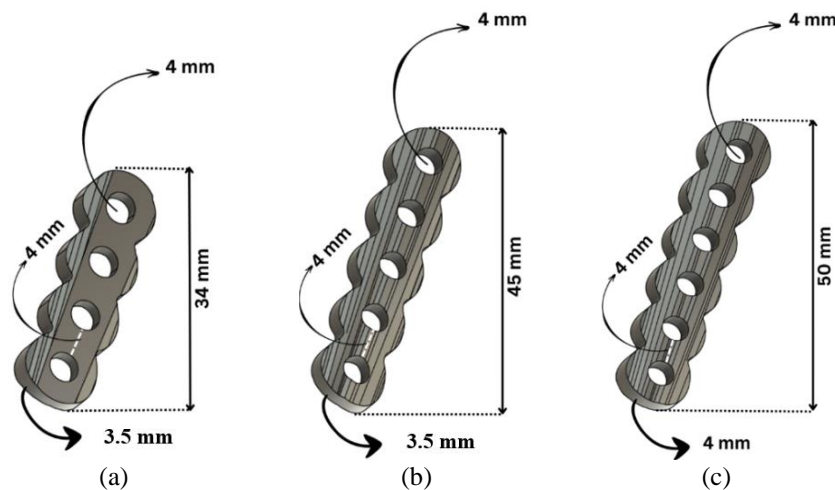


Figure 11. Clavicle plate designs: (a) with 4 holes, (b) with 5 holes, and (c) with 6 holes

Plate design validation was accomplished by simulating plate installation with CNN-based bone segmentation data. PLA filament from a 3D printer is used to create plates, screws, and bones. Implant placement in the clavicle bone requires special care because the installation must be in the position on the portion used when creating the previous implant design so that the position of the implant that is installed is in accordance with the axis. Following the clavicle, 3D printing is used to create implants and screws, which are then implanted on the clavicle. To screw the implant in, the clavicle is first drilled. Figure 12 depicts how the implant appears when it is joined to the clavicle bone with 4 holes in Figure 12(a), 5 holes in Figure 12(b) and 6 holes in Figure 12(c). The experimental test was carried out successfully, as the size and design results of the clavicle implant components are in compliance with the patient's clavicle bone. Screw sizes 18, 18, 18, 16, and 18 mm (beginning from the lateral side) are used for clavicle mounting.

The length of the screw used can vary depending on the location of the implant in a clavicle fracture because it has to adjust the thickness of the clavicle bone, which varies from the lateral to the medial end. If the screw length exceeds 16 mm, the surgeon must pay attention to the screw trajectory and the degree of protrusion of the screw over the clavicle to ensure that the screw remains in a secure area [31]. The clavicle's

anatomical distinctive features require modifications in screw length selection as an aspect in determining drilling depth. According to Qin *et al.* [32] the acromioclavicular joint to the center of the clavicle has a risky drilling angle that will interfere with the subclavian neurovascular, thus this part should be confined to drilling with a maximum depth of 17 mm.

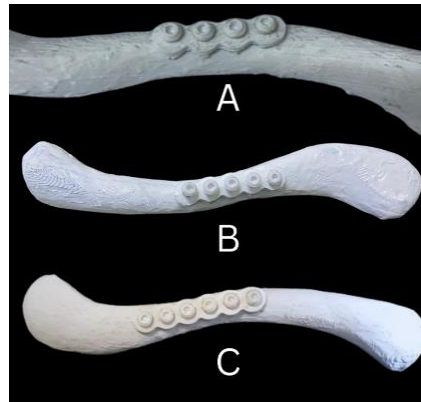


Figure 12. Simulation of the clavicle plate implantation with its screws: (a) for 4 holes, (b) for 5 holes, and (c) for 6 holes

This paper is focused on designing personalized clavicle implants based on the individual patient's clavicle bone surface. In the actual manufacturing process, the industrial company employs advanced fabrication techniques such as CNC machining or 3D printing to create these custom implants [33]. The convolutional neural network method that used in this study is successful in providing the CNN test results of 97.4% for the classification of clavicle bone images. Compared with other research that has carried out the CNN algorithm, such as to classify pneumonia detection on chest X-rays with a final accuracy percentage of 88.14% [34] and research on a new algorithm called improved dial's loading algorithm (IDLA) using a CNN model that combines digital CT image processing and machine learning to identify cancer cells through IDLA automatically with minimum iterations with an accuracy percentage of 92.81% [35], this research improves the results.

In the selection of materials for clavicle bone plate manufacturing, titanium alloy, stainless steel alloy, and cobalt alloy are commonly utilized due to their excellent biocompatibility properties. This paper serves as a valuable resource for recommending suitable materials and design considerations before the fabrication process. Figure 13 illustrates our manufactured clavicle bone plate, highlighting the alignment between the clavicle bone surface and the inner surface of the designed bone plate.



Figure 13. The manufactured clavicle bone plate with metal material selection. The red line emphasizes the match between the clavicle bone surface and the inner surface of the designed bone plate

4. CONCLUSION

The present study demonstrates the implementation of CNN classification in the case of clavicle plate implant design. The clavicle bone has been successfully constructed with assistance using CNN and results in an accuracy of up to 97.4%. As clavicular plate is needed for clavicular fracture treatment on the clavicle bone, the bone plate design in this study has been manufactured and proved to fit in perfectly on the patient's bone contour. CNN classification in this study presents a good, high-speed performance to detect the clavicle bone with high accuracy.

ACKNOWLEDGEMENTS

This research was supported by “Rumah Program Artificial Intelligence, Big Data, dan Teknologi Komputasi (AIBDTK) untuk Biodiversitas dan Citra Satelit OREI 2023, BRIN Indonesia” research fund number B-298/III.6/PR.03/1/2023. The publication fee was supported by Universitas Dian Nuswantoro. The CT-scan data was acquired Saiful Anwar General Hospital and has been permitted by dr. Achmad Bayhaqi Nasir Aslam Sp.Rad.(K). Since the data was considered as secondary data, ethical clearance was not required by the hospital.




REFERENCES

- [1] S. Hyland, M. Charlick, and M. Varacallo, *Anatomy, shoulder and upper limb, clavicle*. 2018.
- [2] R. J. Campbell, C. Handford, M. J. Donaldson, B. S. Sivakumar, E. Jiang, and M. Symes, “Surgical management of clavicle fractures in Australia: an analysis of Australian Medicare Benefits Schedule database from 2001 to 2020,” *ANZ Journal of Surgery*, vol. 93, no. 3, pp. 656–662, Mar. 2023, doi: 10.1111/ans.18312.
- [3] M. Z. Yan *et al.*, “Operative management of midshaft clavicle fractures demonstrates better long-term outcomes: a systematic review and meta-analysis of randomized controlled trials,” *PLOS ONE*, vol. 17, no. 4, Apr. 2022, doi: 10.1371/journal.pone.0267861.
- [4] K. J. Virtanen, V. Remes, J. Pajarinen, V. Savolainen, J.-M. Björkenheim, and M. Paavola, “Sling compared with plate osteosynthesis for treatment of displaced midshaft clavicular fractures,” *Journal of Bone and Joint Surgery*, vol. 94, no. 17, pp. 1546–1553, Sep. 2012, doi: 10.2106/JBJS.J.01999.
- [5] F. Shi, H. Hu, M. Tian, X. Fang, and X. Li, “Comparison of 3 treatment methods for midshaft clavicle fractures: A systematic review and network meta-analysis of randomized clinical trials,” *Injury*, vol. 53, no. 6, pp. 1765–1776, Jun. 2022, doi: 10.1016/j.injury.2022.04.005.
- [6] X. Liu, W. Xu, Q. Xue, and Q. Liang, “Intramedullary nailing versus minimally invasive plate osteosynthesis for distal tibial fractures: a systematic review and meta-analysis,” *Orthopaedic Surgery*, vol. 11, no. 6, pp. 954–965, Dec. 2019, doi: 10.1111/os.12575.
- [7] W. J. Grantham, S. J. Halverson, and D. H. Lee, “Medial clavicle osseous dimensions with implication on plate fixation,” *Techniques in Shoulder & Elbow Surgery*, vol. 20, no. 1, pp. 26–29, Mar. 2019, doi: 10.1097/BTE.0000000000000152.
- [8] L. Wang, K. Guo, K. He, and H. Zhu, “Bone morphological feature extraction for customized bone plate design,” *Scientific Reports*, vol. 11, no. 1, Aug. 2021, doi: 10.1038/s41598-021-94924-9.
- [9] A. Soni and B. Singh, “Design and analysis of customized fixation plate for femoral shaft,” *Indian Journal of Orthopaedics*, vol. 54, no. 2, pp. 148–155, Apr. 2020, doi: 10.1007/s43465-019-00025-1.
- [10] B. Schmutz, K. Rathnayaka, and T. Albrecht, “Anatomical fitting of a plate shape directly derived from a 3D statistical bone model of the tibia,” *Journal of Clinical Orthopaedics and Trauma*, vol. 10, pp. S236–S241, 2019, doi: 10.1016/j.jcot.2019.04.019.
- [11] C. E. Cardenas, J. Yang, B. M. Anderson, L. E. Court, and K. B. Brock, “Advances in auto-segmentation,” *Seminars in Radiation Oncology*, vol. 29, no. 3, pp. 185–197, Jul. 2019, doi: 10.1016/j.semradonc.2019.02.001.
- [12] A. Musha, A. Al Mamun, A. Tahabilder, M. J. Hossen, B. Hossen, and S. Ranjbari, “A deep learning approach for COVID-19 and pneumonia detection from chest X-ray images,” *International Journal of Electrical and Computer Engineering (IJECE)*, vol. 12, no. 4, Aug. 2022, doi: 10.11591/ijece.v12i4.pp3655-3664.
- [13] C. Kim, D. Kim, H. Jeong, S.-J. Yoon, and S. Youm, “Automatic tooth detection and numbering using a combination of a CNN and heuristic algorithm,” *Applied Sciences*, vol. 10, no. 16, Aug. 2020, doi: 10.3390/app10165624.
- [14] A. Borjali *et al.*, “Comparing the performance of a deep convolutional neural network with orthopedic surgeons on the identification of total hip prosthesis design from plain radiographs,” *Medical Physics*, vol. 48, no. 5, pp. 2327–2336, May 2021, doi: 10.1002/mp.14705.
- [15] Y. Qu *et al.*, “Surgical planning of pelvic tumor using multi-view CNN with relation-context representation learning,” *Medical Image Analysis*, vol. 69, Apr. 2021, doi: 10.1016/j.media.2020.101954.
- [16] K. J. Kim, D. H. Kim, J. Il Lee, B. K. Choi, I. H. Han, and K. H. Nam, “Hounsfield units on lumbar computed tomography for predicting regional bone mineral density,” *Open Medicine*, vol. 14, no. 1, pp. 545–551, Jul. 2019, doi: 10.1515/med-2019-0061.
- [17] C. Andriesei, “Experiments to assess the implementation of a 4 GHz proximity detector for smart crosswalk,” in *2020 13th International Conference on Communications (COMM)*, Jun. 2020, pp. 359–362, doi: 10.1109/COMM48946.2020.9141951.
- [18] M. S. I. Prottasha and S. M. S. Reza, “A classification model based on depthwise separable convolutional neural network to identify rice plant diseases,” *International Journal of Electrical and Computer Engineering (IJECE)*, vol. 12, no. 4, pp. 3642–3654, Aug. 2022, doi: 10.11591/ijece.v12i4.pp3642-3654.
- [19] Ó. Gómez, P. Mesejo, and Ó. Ibáñez, “Automatic segmentation of skeletal structures in X-ray images using deep learning for comparative radiography,” *Forensic Imaging*, vol. 26, Sep. 2021, doi: 10.1016/j.fri.2021.200458.
- [20] O. Gómez, P. Mesejo, O. Ibáñez, A. Valsecchi, and O. Córdón, “Deep architectures for high-resolution multi-organ chest X-ray image segmentation,” *Neural Computing and Applications*, vol. 32, no. 20, pp. 15949–15963, Oct. 2020, doi: 10.1007/s00521-019-04532-y.
- [21] ISO, *ISO 5835:1991. Implants for surgery — Metal bone screws with hexagonal drive connection, spherical under-surface of head, asymmetrical thread — Dimensions*, 2022.
- [22] V. Tongel, D. W. A., Y. L., Shimamura, J. Sijbers, and T. Huysmans, “Fracture patterns in midshaft clavicle fractures,” *Acta Orthopædica Belgica*, vol. 87, no. 3, pp. 501–507, 2021.
- [23] S. Zhu, J. Huang, X. Zhang, X. Zhang, and X. Tong, “Backstepping based nonlinear control for the modular multilevel converter to against parameters variation,” in *2019 14th IEEE Conference on Industrial Electronics and Applications (ICIEA)*, Jun. 2019, pp. 2254–2259, doi: 10.1109/ICIEA.2019.8834379.
- [24] S. Kaur, R. Hooda, A. Mittal, Akashdeep, and S. Sofat, “Deep CNN-based method for segmenting lung fields in digital chest radiographs,” in *Advanced Informatics for Computing Research: First International Conference, ICAICR 2017*, 2017, pp. 185–194, doi: 10.1007/978-981-10-5780-9_17.
- [25] S. R. Dubey, S. K. Singh, and B. B. Chaudhuri, “Activation functions in deep learning: A comprehensive survey and benchmark,” *Neurocomputing*, vol. 503, pp. 92–108, Sep. 2022, doi: 10.1016/j.neucom.2022.06.111.




- [26] H. Pratiwi *et al.*, “Sigmoid activation function in selecting the best model of artificial neural networks,” *Journal of Physics: Conference Series*, vol. 1471, no. 1, Feb. 2020, doi: 10.1088/1742-6596/1471/1/012010.
- [27] J. Qi *et al.*, “Biomechanical testing of three coracoclavicular ligament reconstruction techniques with a 3D printing navigation template for clavicle-coracoid drilling,” *Annals of Translational Medicine*, vol. 9, no. 14, pp. 1121–1121, Jul. 2021, doi: 10.21037/atm-21-737.
- [28] R. Cheng, Z. Jiang, D. Dimitriou, W. Gong, and T.-Y. Tsai, “Biomechanical analysis of personalised 3D-printed clavicle plates of different materials to treat midshaft clavicle fractures,” *Journal of Shanghai Jiaotong University (Science)*, vol. 26, no. 3, pp. 259–266, Jun. 2021, doi: 10.1007/s12204-021-2291-7.
- [29] A. D. Fontana *et al.*, “The variance of clavicular surface morphology is predictable: an analysis of dependent and independent metadata variables,” *JSES International*, vol. 4, no. 3, pp. 413–421, Sep. 2020, doi: 10.1016/j.jseint.2020.05.004.
- [30] N. Samala and B. Manasa, “Sex determination using anthropometric dimensions of clavicle-an observational study,” *International Journal of Anatomy Radiology & Surgery*, vol. 8, no. 1, pp. 24–26, 2019, doi: 10.7860/IJARS/2019/37954:2455.
- [31] H. S. Clitherow and G. Bain, “Association between screw prominence and vascular complications after clavicle fixation,” *International Journal of Shoulder Surgery*, vol. 8, no. 4, 2014, doi: 10.4103/0973-6042.145261.
- [32] D. Qin, Q. Zhang, Y.-Z. Zhang, J.-S. Pan, and W. Chen, “Safe drilling angles and depths for plate-screw fixation of the clavicle: Avoidance of inadvertent iatrogenic subclavian neurovascular bundle injury,” *Journal of Trauma: Injury, Infection & Critical Care*, vol. 69, no. 1, pp. 162–168, Jul. 2010, doi: 10.1097/TA.0b013e318181bbd617.
- [33] J. S. Park *et al.*, “Plate fixation versus titanium elastic nailing in midshaft clavicle fractures based on fracture classifications,” *Journal of Orthopaedic Surgery*, vol. 28, no. 3, May 2020, doi: 10.1177/2309499020972204.
- [34] O. A. Fagbuagun, O. Nwankwo, S. A. Akinpelu, and O. Folorunsho, “Model development for pneumonia detection from chest radiograph using transfer learning,” *TELKOMNIKA (Telecommunication Computing Electronics and Control)*, vol. 20, no. 3, Jun. 2022, doi: 10.12928/telkomnika.v20i3.23296.
- [35] N. S. Reddy and V. Khanaa, “Intelligent deep learning algorithm for lung cancer detection and classification,” *Bulletin of Electrical Engineering and Informatics (BEEI)*, vol. 12, no. 3, pp. 1747–1754, Jun. 2023, doi: 10.11591/eei.v12i3.4579.

BIOGRAPHIES OF AUTHORS






Dita Ayu Mayasari    graduate with a biomedical engineering bachelor’s degree at Airlangga University in 2014 and a Master of Biotechnology from the University of Gajah Mada in 2016. She is working as a lecturer in the Department of Biomedical Engineering, Dian Nuswantoro University, Indonesia. Her interest is in biomechanics, biomaterials, medical rehabilitation technology and assistive technology. She can be contacted at email: mayasari.dita@dsn.dinus.ac.id.






Ihtifazhuddin Hawari    graduate in 2019 from University of Dian Nuswantoro Semarang as Bachelor of Engineering, majoring in electrical engineering with concentration computer engineering. Currently, he is a laboratory staff in the Faculty of Engineering, Dian Nuswantoro University. His main research interest is artificial intelligence research. He can be contacted at email: ihtifazhuddin.hawari@adm.dinus.ac.id.






Sheba Atma Dwiyantri    graduated in 2022 from Dian Nuswantoro University Semarang-Indonesia, with a major in biomedical engineering. She works as a laboratory assistant in the Biomedical Engineering Laboratory at Dian Nuswantoro University. Her research interest is image processing includes 3D reconstruction, implant planning, and the healthcare system. She can be contacted at email: 513201800040@mhs.dinus.ac.id.






Nathasya Reinelda Noviyadi    is a student in undergraduate program of Biomedical Engineering at Dian Nuswantoro University, Semarang, Indonesia. She works as a teaching assistant in the Biomedical Engineering Laboratory at Dian Nuswantoro University. Her research interests are clavicle implants, including design, finite element testing, and healthcare systems. She can be contacted at email: 51320202000132@mhs.dinus.ac.id.






Dinda Syaqila Andryani    is a student in undergraduate program of Biomedical Engineering at Dian Nuswantoro University, Semarang, Indonesia. She works as a laboratory assistant in the Biomedical Engineering Laboratory at Dian Nuswantoro University. Her research interest is bone implants design and artificial intelligence. She can be contacted at email: dindasaqila9@gmail.com.






Muhammad Satrio Utomo    received a Bachelor of Engineering in Mechanical Engineering major in 2012 from the University of Indonesia, Depok, Indonesia. He has completed her MS degree in 2015 from biomedical engineering at the Wayne State University, United State of America. He is studying as a doctoral student in the Department of Biomedical Engineering, University of Melbourne, Australia. Besides employed as an early career researcher in the Research Center for Metallurgy, National Research and Innovation Agency, Indonesia, he was also lecturer in the medical technology cluster at the Faculty of Medicine in the University of Indonesia. He can be contacted at email: muha176@brin.go.id and muut@unimelb.au.edu.



Nada Fitriyatul Hikmah    earned her bachelor's degree in biomedical engineering from Airlangga University (UNAIR) in 2012. She then pursued her master's education in electrical engineering-electronics, specializing in biomedical engineering, at the Sepuluh Nopember Institute of Technology (ITS) and earned her master's degree in 2016. Currently, she works as a lecturer at the Department of Biomedical Engineering, Faculty of Electrical Technology and Intelligent Informatics, ITS, Indonesia. Her research interests include cardiac engineering, signal processing, and medical imaging. She can be contacted at email: nadafh@bme.its.ac.id.



Talitha Asmaria    received a Bachelor of Engineering in biomedical Engineering major in 2012 from Airlangga University, Surabaya, Indonesia. She has completed her MSc degree in 2016 from biomedical engineering at the University of Bristol, United Kingdom. She is currently an early career researcher in the Center of Biomedical Research, National Research and Innovation Agency, Indonesia. Her research interest is the implant planning, which includes design analysis, image processing, material development, and 3D printing technology. She can be contacted at email: talitha.asmaria@brin.go.id.